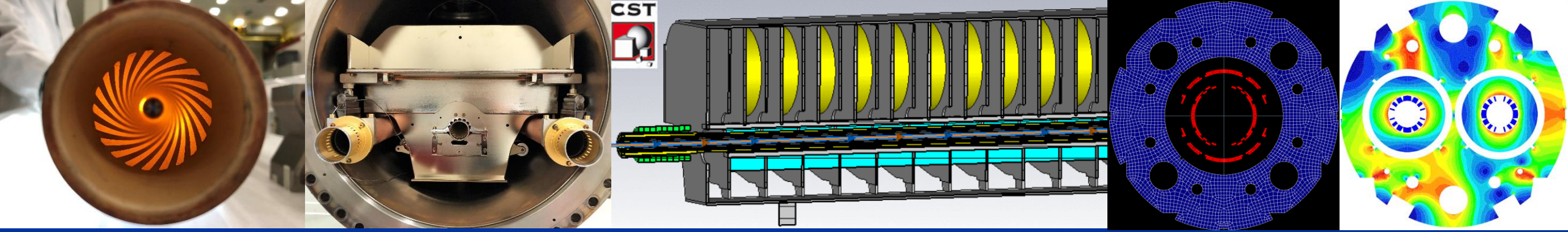

Analysis, simulations and measurements for the operation of accelerator magnets

Agnieszka Chmielińska

PE Section Meeting

09.11.2023

Career history

Oct. 2010 – Feb. 2014

B.Sc. in Applied Physics
AGH-UST & TE-VSC Trainee Student
- *Simulations and tests of the ion pump controller electronic system*

Mar. 2014 – Apr. 2016

M.Sc. in Applied Physics
AGH-UST & TE-VSC Technical Student
- *Secondary-electron yield measurements at cryogenic temperatures*
- *Analysis of surface conditioning to better understand the electron-cloud effect*

Aug. 2016 – Dec. 2019

Ph.D. in Physics
EPFL & TE-ABT Doctoral Student
- *Development of a novel beam screen for kicker magnets, involving EM simulations, electric-circuit simulations and RF measurements*

Sept. 2020 – Aug. 2023

Senior Fellow
CERN, TE-MSC
- *EM simulations of superconducting magnets and design of experiments*
- *Software design and implementation for data-processing in automated workflows*
- *Magnetic field prediction for operation*

Doctoral Student in TE-ABT-PPE (2016-2019)

Optimization of the beam screen for the FCC injection kicker magnets, Ph.D. at EPFL (2019)

- Contribution to the **upgrade** and **commissioning** of the LHC Injection Kicker Magnet (LHC MKI)

- Development of the **novel concept** of a **helical beam screen**
  - Improved high-voltage performance
  - Reduced beam-coupling impedance

Conceptual design

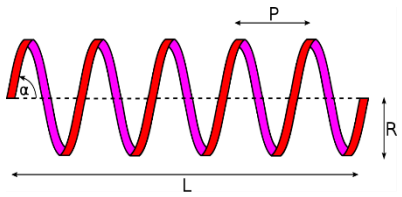

Electric-circuit simulations (Cadence PSpice)

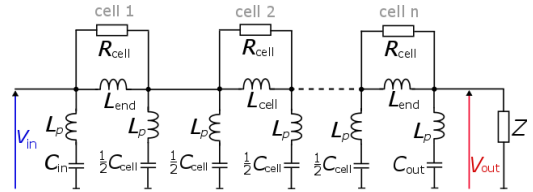

EM simulations (CST Studio Suite, Opera-2D)

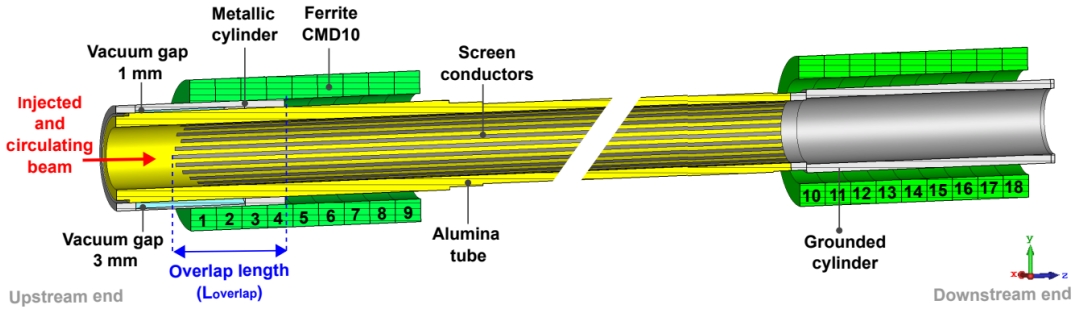

RF measurements (LHC MKI) and signal processing

Prototype validation

Beam screen for the kicker magnets

Introduction

CERN accelerator complex:

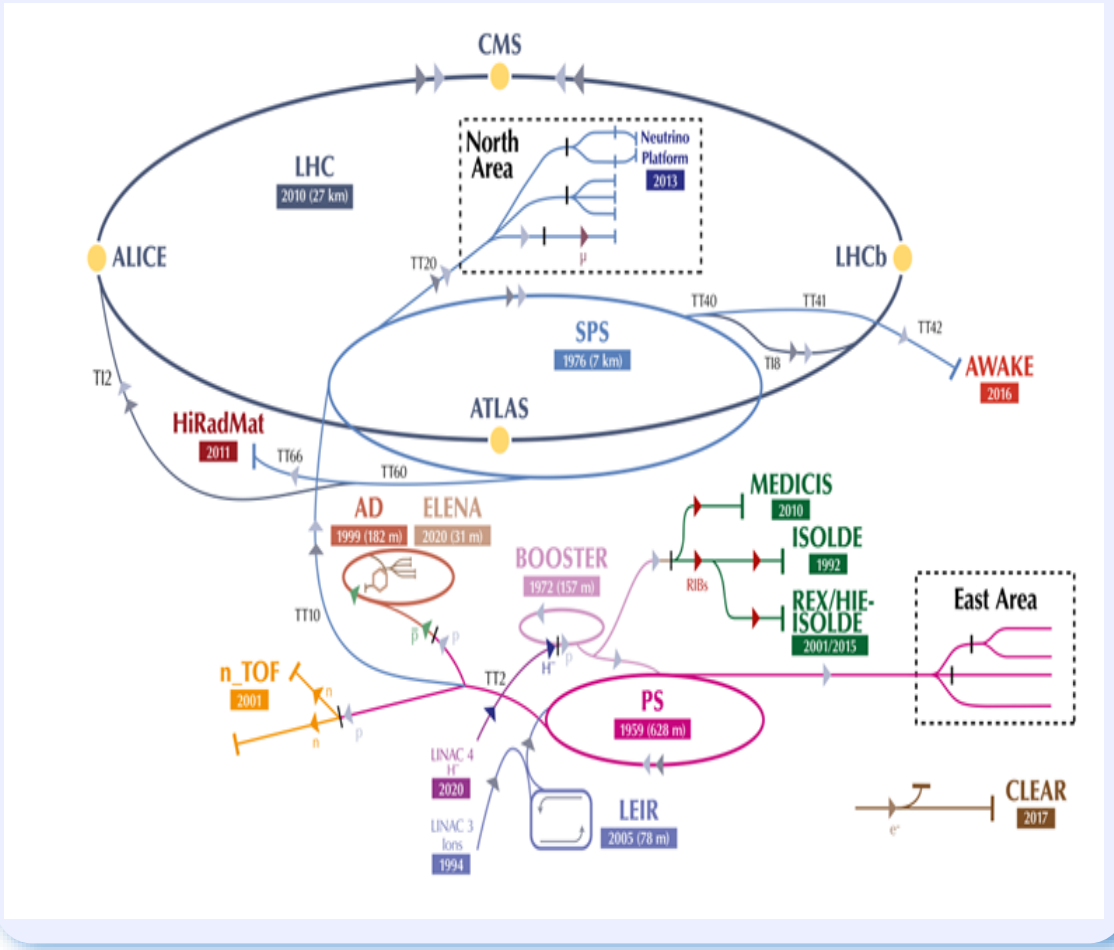

What do we mean by **injection**?

A particle beam must be injected into a circular accelerator or accumulator **at the right time** while**:**

- placing the newly injected particles onto the **correct trajectory,**
- **minimizing beam loss.**

Machine protection related issues:

- **high beam energy** (up to 2.4 MJ for each LHC injection and twice more for FCC-hh).

Technological challenges:

- fast, high voltage **pulse generators**,
- special types of magnets (**kickers** and septa).

Injection kicker magnet (I)

Single-turn injection:

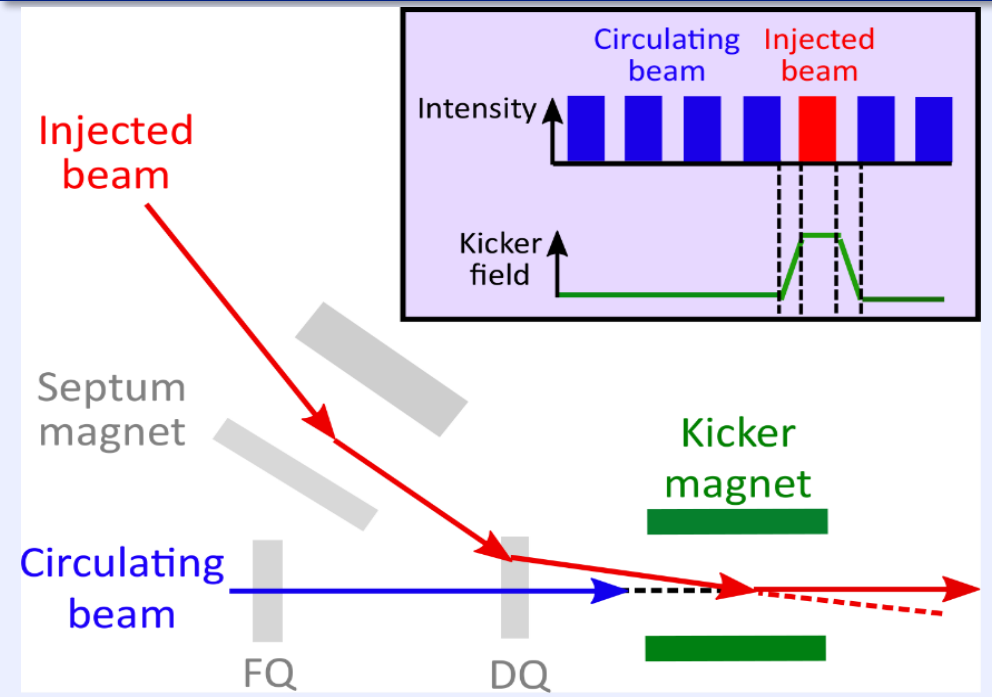

- **Kicker magnet** is a pulsed dipole magnet with very **fast rise and/or fall time** (from tens to hundreds of nanoseconds)
- It “sees” the circulating beam!

C-core ferrite:

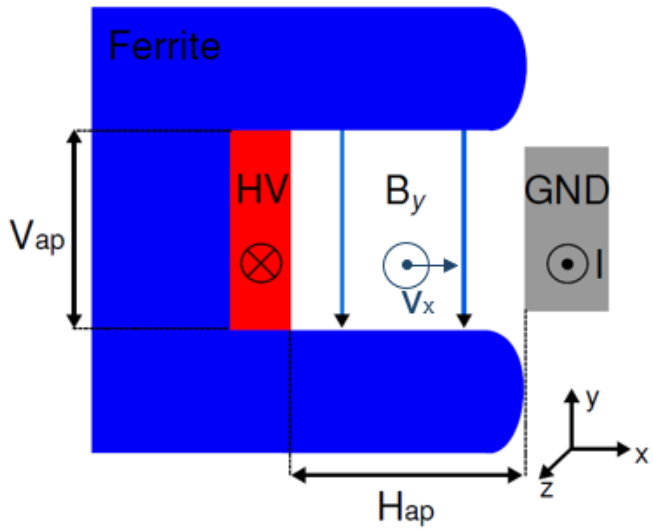

- **Ni-Zn ferrite yoke** is always used for fast applications (e.g. 8C11, CMD5005)

Injection kicker magnet (II)

Transmission line ferrite-loaded kicker magnet is the best option to achieve fast field rise and fall times with low pulse ripple.

Transmission line topology:

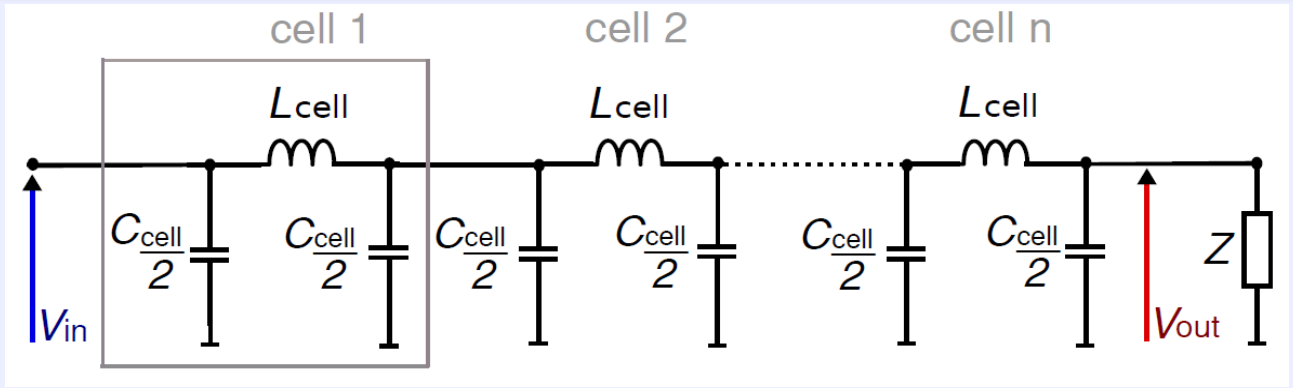

- **Complicated design**
- **Field rise time** (τ_r) depends on pulse propagation time through the magnet:

$$\tau_m = n\sqrt{L_{\text{cell}}C_{\text{cell}}} = n\frac{L_{\text{cell}}}{Z}$$

- **Fast:** field rise times $\ll 1$ µs

Field rise time:

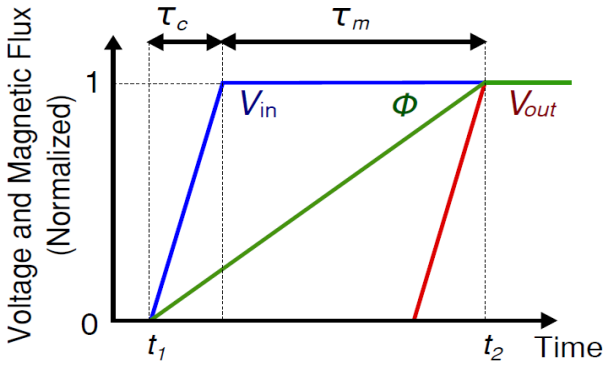

- **Magnetic flux:**

$$\Phi = \int (V_{\text{in}} - V_{\text{out}})dt$$

- **Field rise time:**

$$\tau_r \sim \tau_m + \tau_c$$

τ_c – rise time of the voltage pulse

Example: LHC injection kicker magnet (MKI)

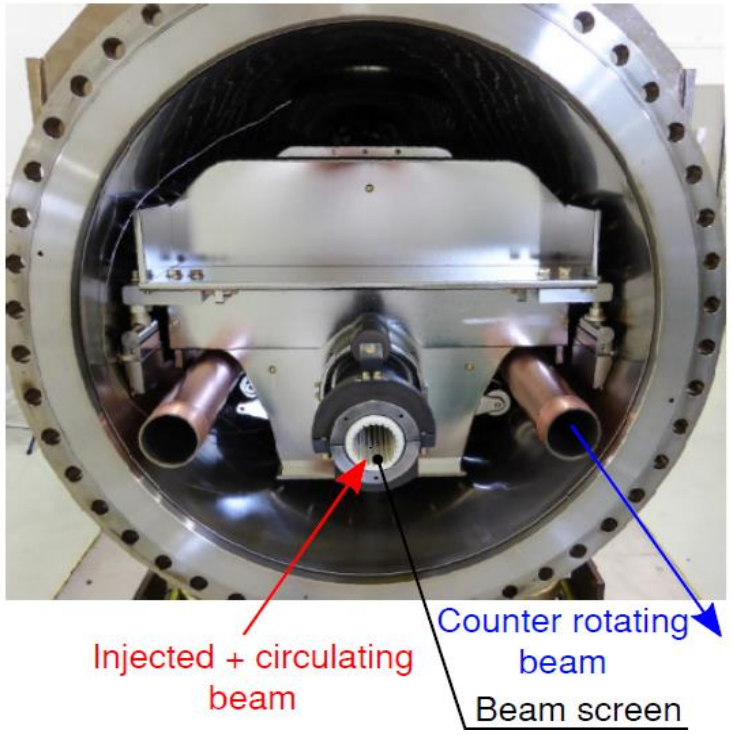

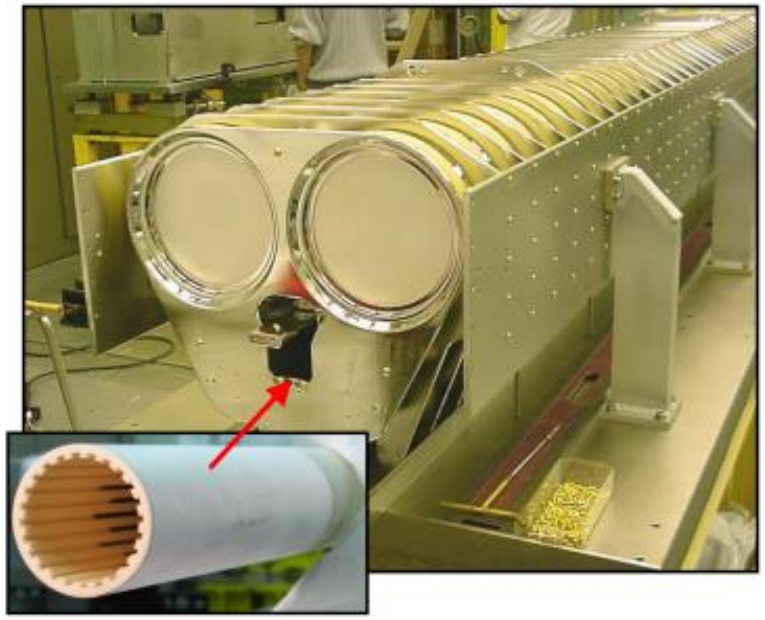

Parameter	Value	Unit
Number of magnets per system	4	-
Kicker strength per magnet	0.3	T·m
Number of cells per magnet	33	-
Characteristic impedance	5	Ω
Designed magnet voltage	27	kV
Aperture height/width	54/54	mm
Magnetic field flat-top duration	up to 7.86	μs
Designed field rise time 0.5%-99.5%	0.9	μs
Designed field fall time 99.5%-0.5%	3	μs
Beam screen inside diameter	38	mm
Magnet length	2.7	m

Major problem: **beam-induced heating** due to the **real component of the longitudinal beam-coupling impedance** → a **beam screen** is placed in the aperture of each LHC MKI.

Beam coupling impedance

Reference system:

The wake field generated by the source particle affects the witness particle.

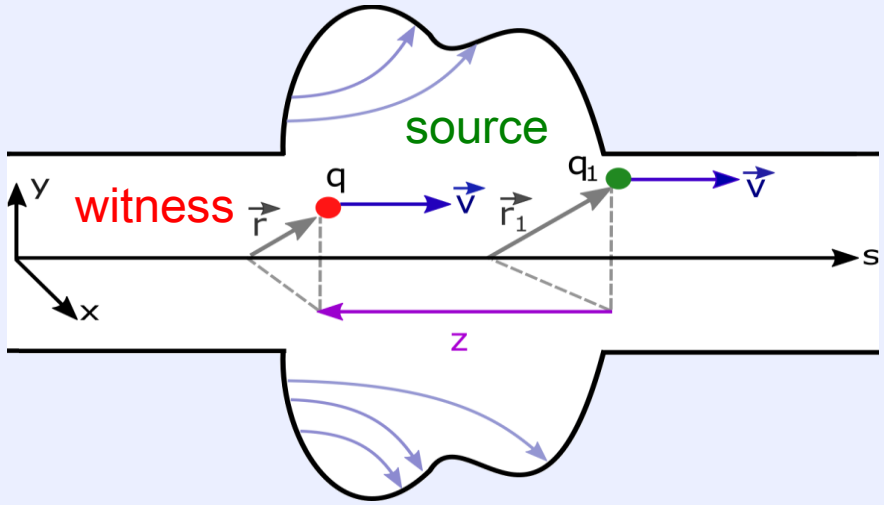

The net force acting on the witness charge:

$$\vec{F}(\vec{r}_1, s_1, \vec{r}, s, t) = q\left[\vec{E}(\vec{r}_1, s_1, \vec{r}, s, t) + \vec{v} \times \vec{B}(\vec{r}_1, s_1, \vec{r}, s, t)\right]$$

$$\vec{F}(\vec{r}_1, s_1, \vec{r}, s, t) = \vec{F}_{\parallel} + \vec{F}_{\perp}$$

Longitudinal wake function:

$$W_{\parallel}(z) = -\frac{1}{q_1 q}\int_0^L \vec{F}_{\parallel}(\vec{r}_1, s_1, \vec{r}, s, t)_{|t=\frac{s-z}{\beta c}, s_1=s-z} ds.$$

$$W_{\parallel}(z) = -\frac{\Delta E(\vec{r}_1, \vec{r}, z)}{q_1 q}.$$

Longitudinal beam coupling impedance:

$$Z_{\parallel}(\omega) = \frac{1}{\beta c}\int_{-\infty}^{+\infty} W_{\parallel}(z) e^{j\omega\frac{z}{\beta c}} dz.$$

What happens to the energy lost by the source?

- Partially dissipates in the walls or HOM absorbers:
  → Heat load
- Partially transferred to the following particles
  → Beam instabilities

Beam-induced heating

Power loss (multipole pass):

$$P = -2(qN_pN_bf_0)^2\left[\left(\sum_{p=1}^{+\infty}\left|\hat{\lambda}_{\mathrm{beam}}(p\omega_0)\right|^2 \mathrm{Re}\left[Z_{\parallel}(p\omega_0)\right]\right) + \tfrac{1}{2}\left|\hat{\lambda}_{\mathrm{beam}}(0)\right|^2 \mathrm{Re}\left[Z_{\parallel}(0)\right]\right]$$

N_b – number of bunches, N_p– bunch intensity, f_0 – revolution frequency, $\hat{\lambda}_{\mathrm{beam}}$ – beam spectrum.

Beam spectrum

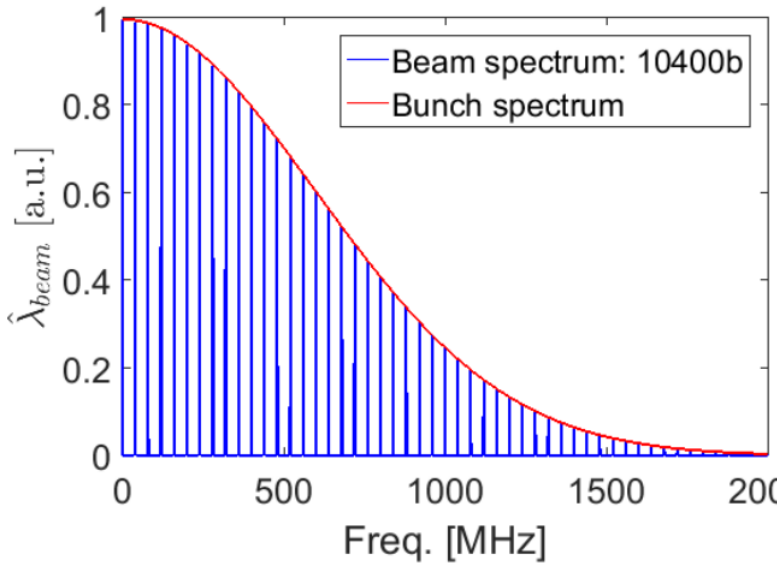

25 ns bunch spacing → 40 MHz beam harmonics

Impedance spectrum

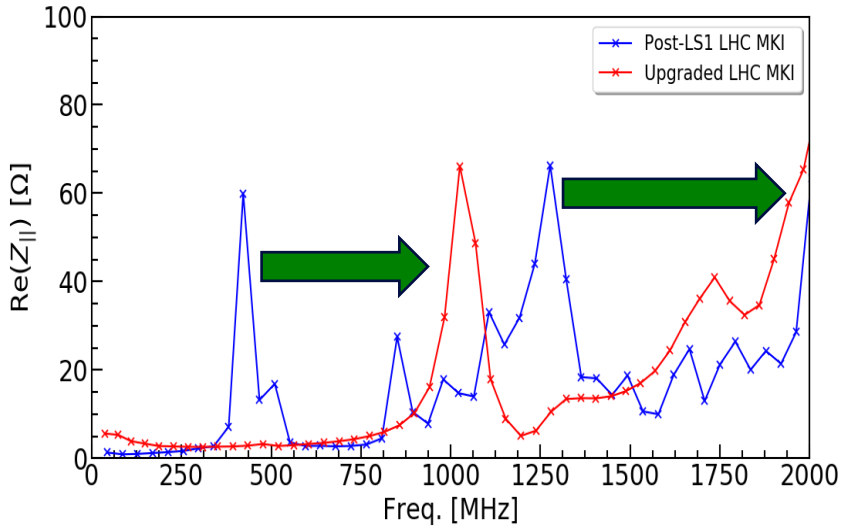

Shift the peaks towards higher frequencies!

Consequences:

For high-intensity beams, heating of the ferrite yoke can result in:

→ local vacuum degradation

→ loss of the magnetic properties (Curie point exceeded)

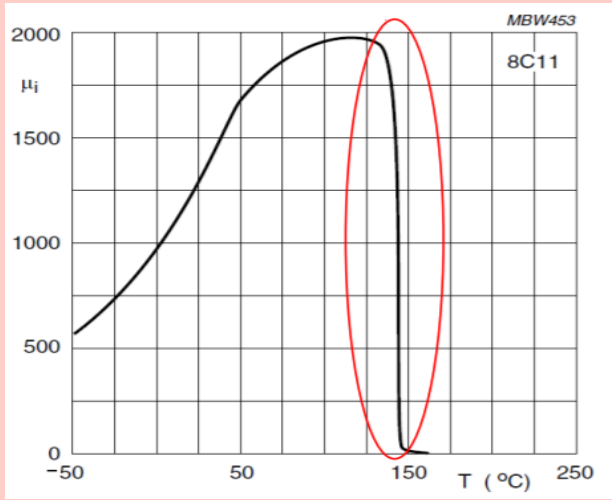

Beam screening: Conventional design (I)

LHC MKI post-LS1 beam screen:

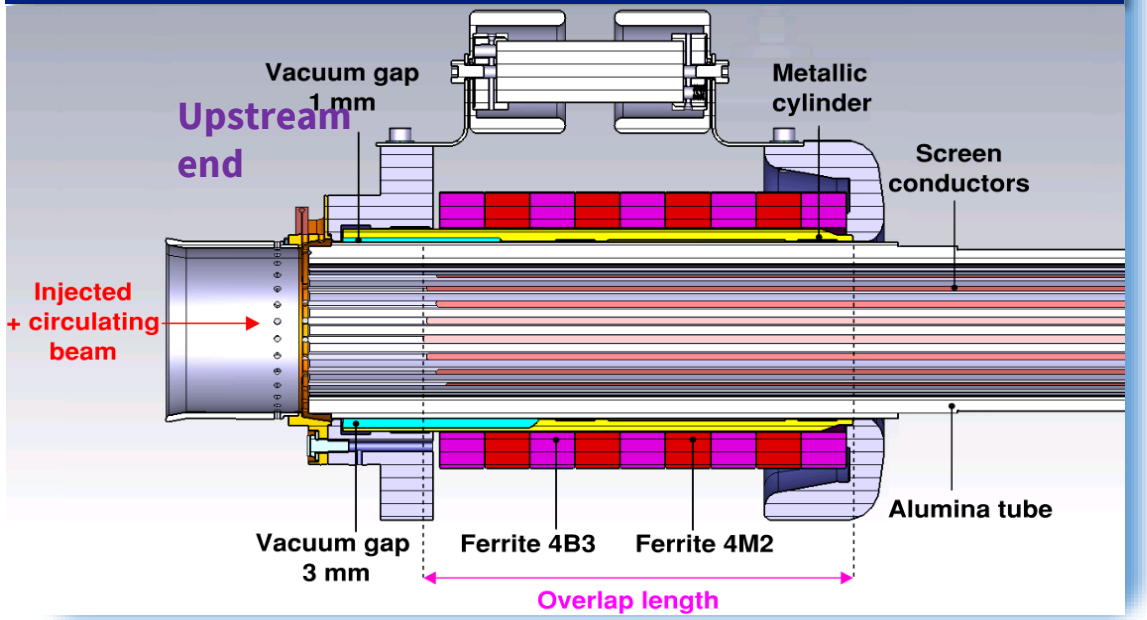

More than 15 years of development…

General features:

- **24 (NiCr) straight screen conductors**
  → **reduced beam coupling impedance**
- **Capacitive coupling** to the beam pipe at the upstream end and connection to the beam pipe at the downstream end
  → **fast magnetic field rise time**
- **Overlap length** determines resonances in the longitudinal impedance spectrum
  → **possibility to shift resonant modes to higher frequencies:**

$$f_{\mathrm{conv}}^{(n)} = \frac{nc}{2\sqrt{\varepsilon_{r,\mathrm{eff}}}+(L_{\mathrm{overlap}}+\delta_{\mathrm{fringe}})}$$

- **Ferrite rings** at both ends of the beam screen
  → **power loss reduction in the ferrite yoke**

Beam screening: Conventional design (II)

During magnetic field rise and fall, a significant voltage is induced on the screen conductors.

→ Possibility of HV breakdowns

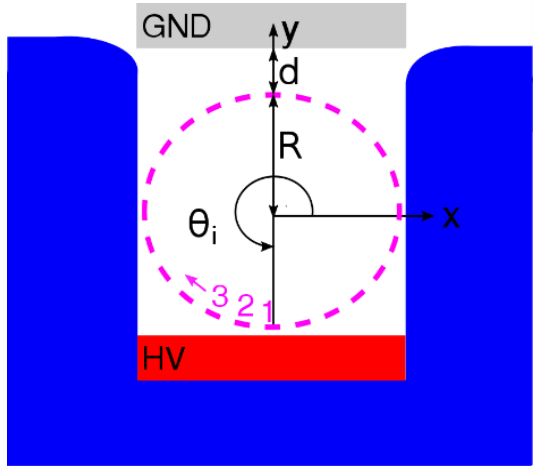

Induced voltage:

$$V_i = \frac{d\Phi}{dt} = \frac{dB}{dt}(d + R - y_i)L$$

Magnet voltage and voltage of screen conductor:

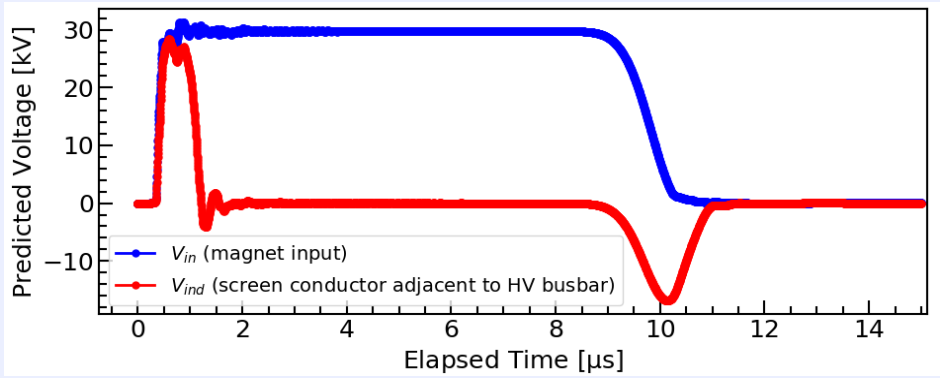

Maximum conductor and inter-conductor voltages (for 60 kV PFN voltage):

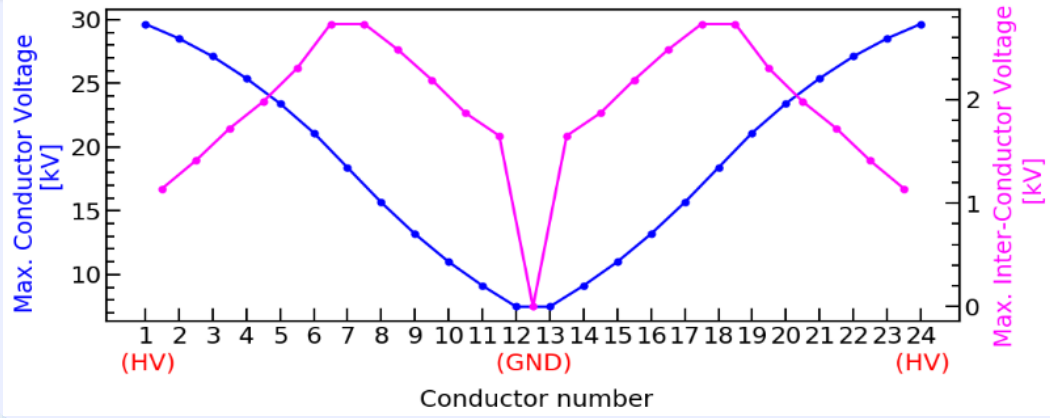

Design of a beam screen for FCC-hh

1. Analysis of the LHC MKI beam screen *(not discussed here)*
2. Design of the conventional beam screen for FCC-hh *(not discussed here)*
3. Development of a novel helical beam screen for FCC-hh *(next slides)*

Design of a kicker magnet module for FCC-hh

Specification of baseline parameters

↓

PSpice model

↓

Analysis of field rise time and field flat-top quality

↓

CST model

Analysed kicker waveform:

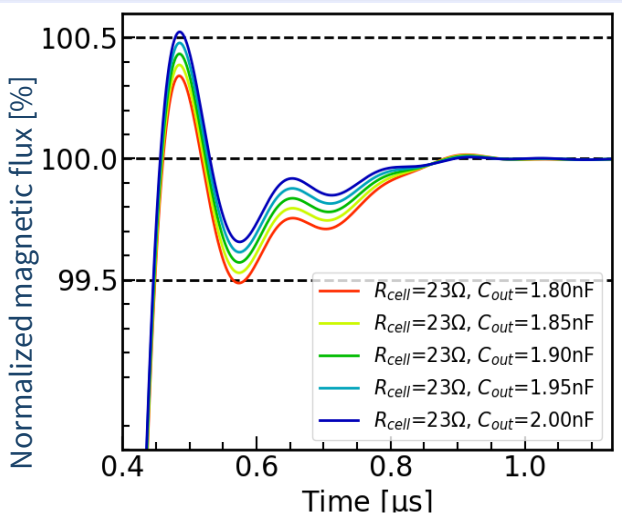

Baseline parameters:

Injecton energy [TeV]	3.3
Angle [mrad]	0.18
Pulse duration [µs]	2
Current [kA]	2.4
Voltage [kV]	15
System impedance [Ω]	6.25
System length [m]	40
Field rise time [µs]	0.43
Aperture dimensions [mm]	48/48
Magnet fill time [µs]	0.355
Good field region (h/v) [mm]	8/8
Flat-top tolerance [%]	±0.5

18 magnets per injection system

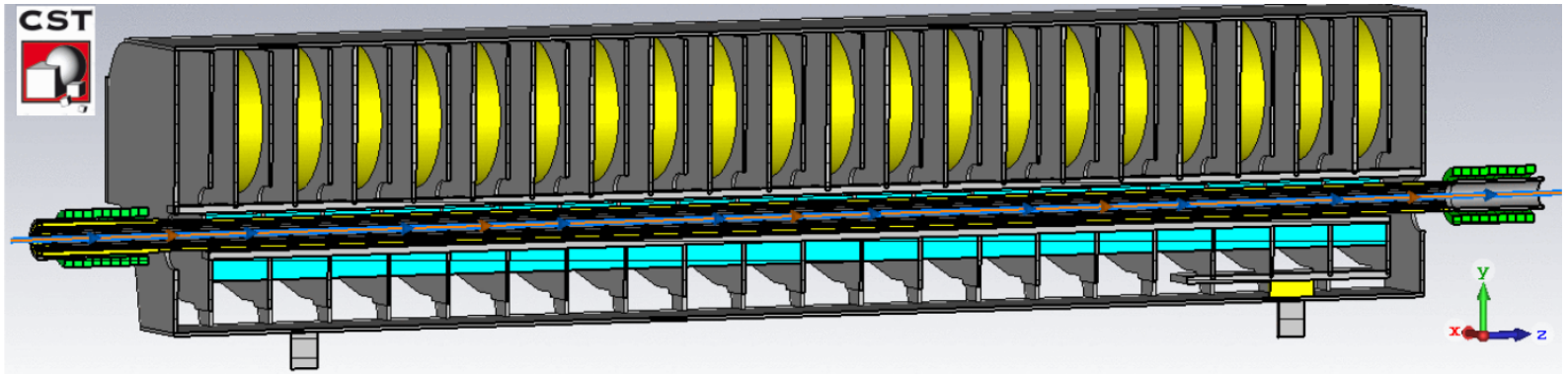

New PSpice model and CST model

Power deposition estimates

Unshielded kicker magnet:

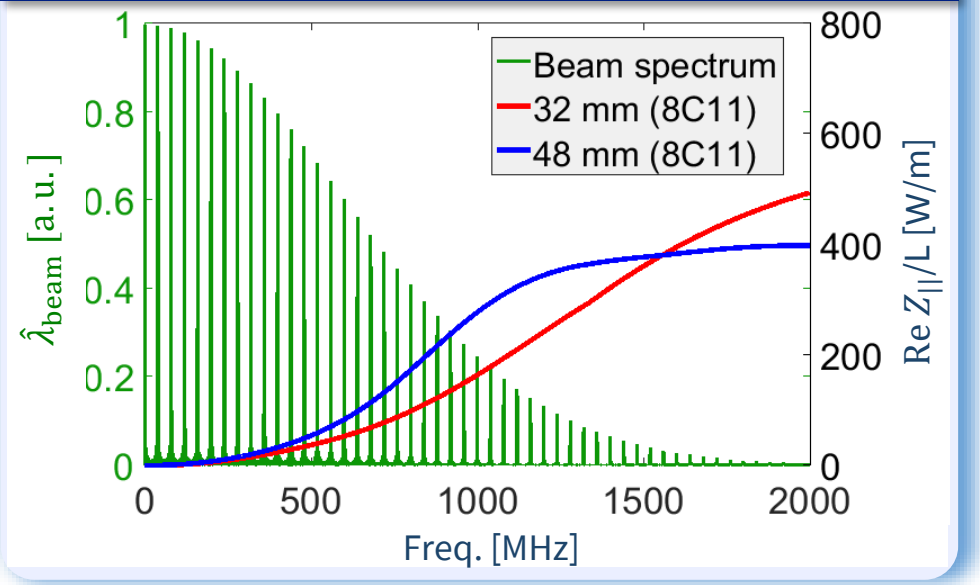

Aperture dimensions [mm x mm]	P [W/m] Ideal beam spectrum	P [W/m] Nominal beam spectrum
32 x 32	227.1	228.1
48 x 48	353.9	355.4

LHC MKI limit: 160 W/m.

Power loss is at unacceptable level.

Kicker magnet with the conventional beam screen:

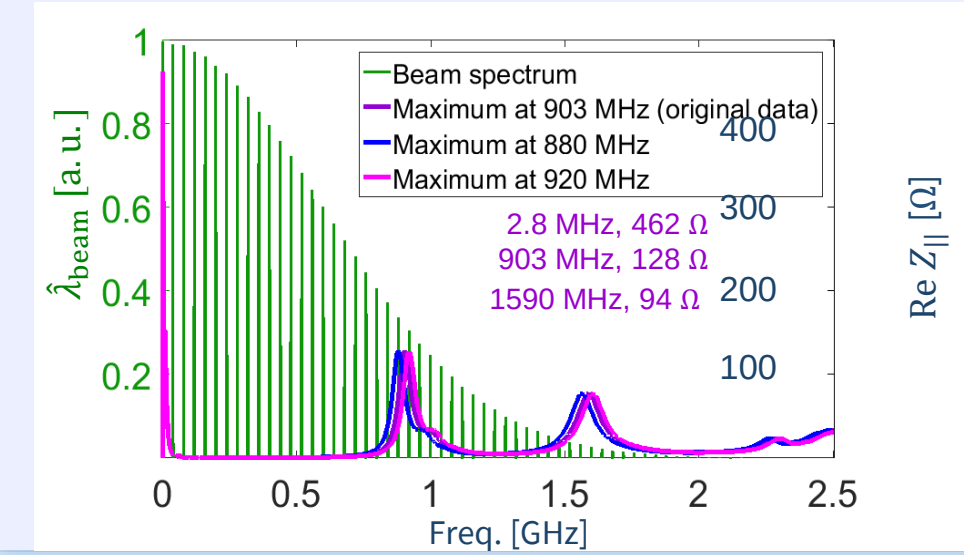

Worst case scenario: 30.2 W/33.4 W/29.3 W

→ significant reduction in comparison with unshielded kicker (P~355 W/m),

→ lower than for the upgraded LHC MKI8D.

New concept of a helical beam screen

Each screen conductor has a form of a helix:

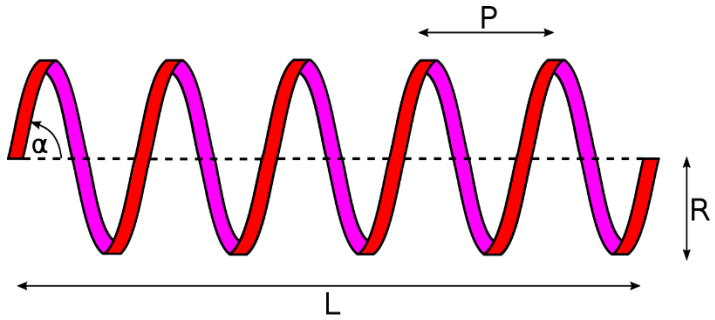

Photograph of the alumina tube with 21 screen conductors applied using Ag paint

Induced voltage:

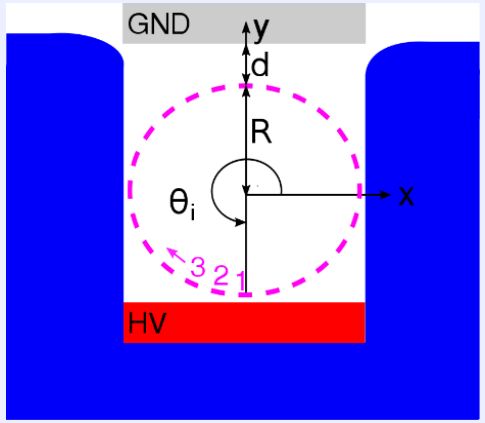

For an **integer number** of turns:

$$V_i = \frac{dB}{dt}(d + R)L$$

→ **the same induced voltage on each conductor**

→ this is **one-half** of the worst-case voltage induced on a straight conductor.

Significantly improved HV performance

Beam coupling impedance simulations

- Beam coupling impedance modelling (CST Studio Suite) to optimize:
  - **Beam-induced heating**
  - **Power distribution**
  - **Impact on beam stability**

No heating issues are expected for the FCC-hh kicker magnets for nominal beam parameters.

Longitudinal impedance optimization

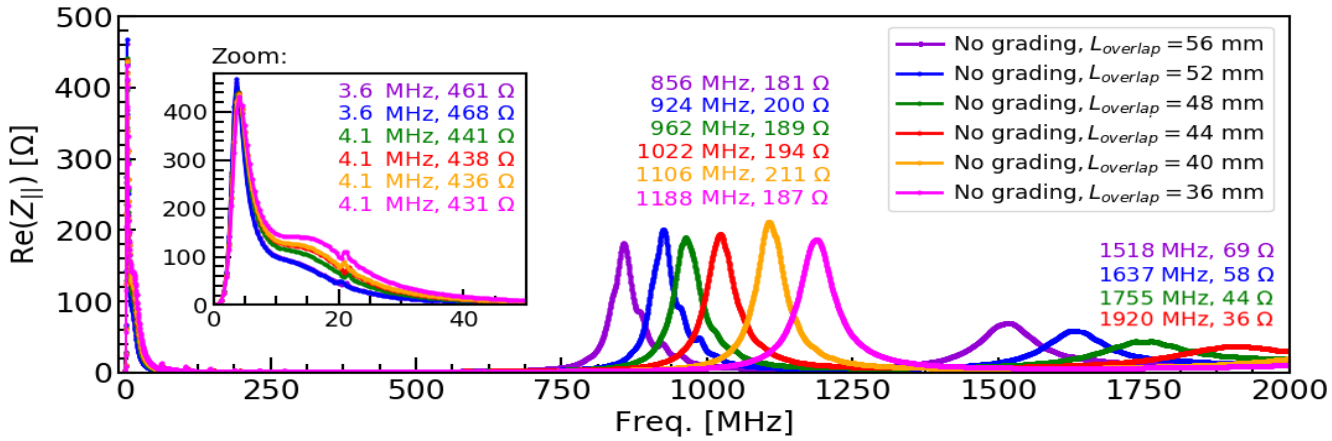

Power deposition distribution

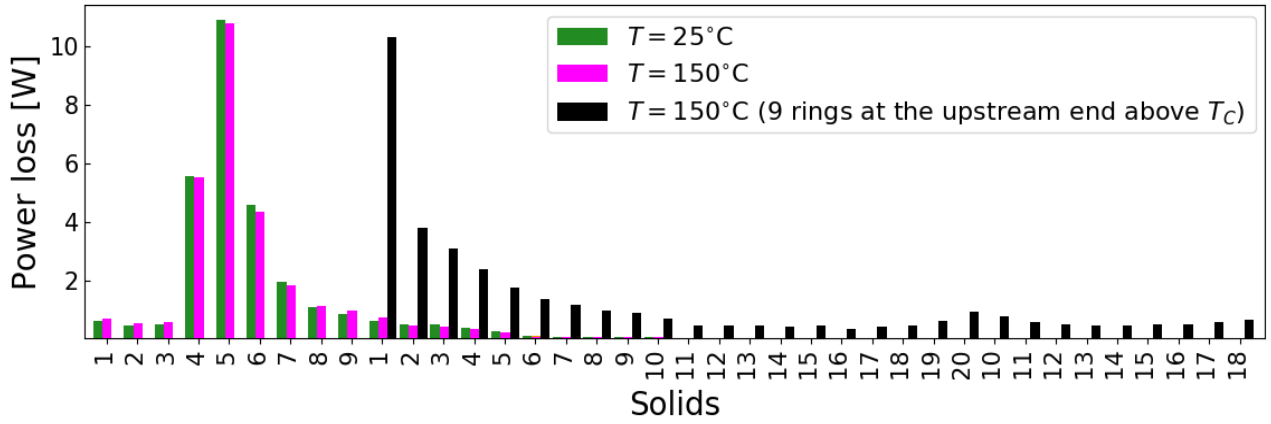

Characterization of EM properties of ferrites

- Novel measurements of EM properties of ferrites as a function of **frequency** and **temperature** (short-circuit line method):
  → new input for beam impedance simulations.

Measured temperature dependence complex permeability for CMD5005.

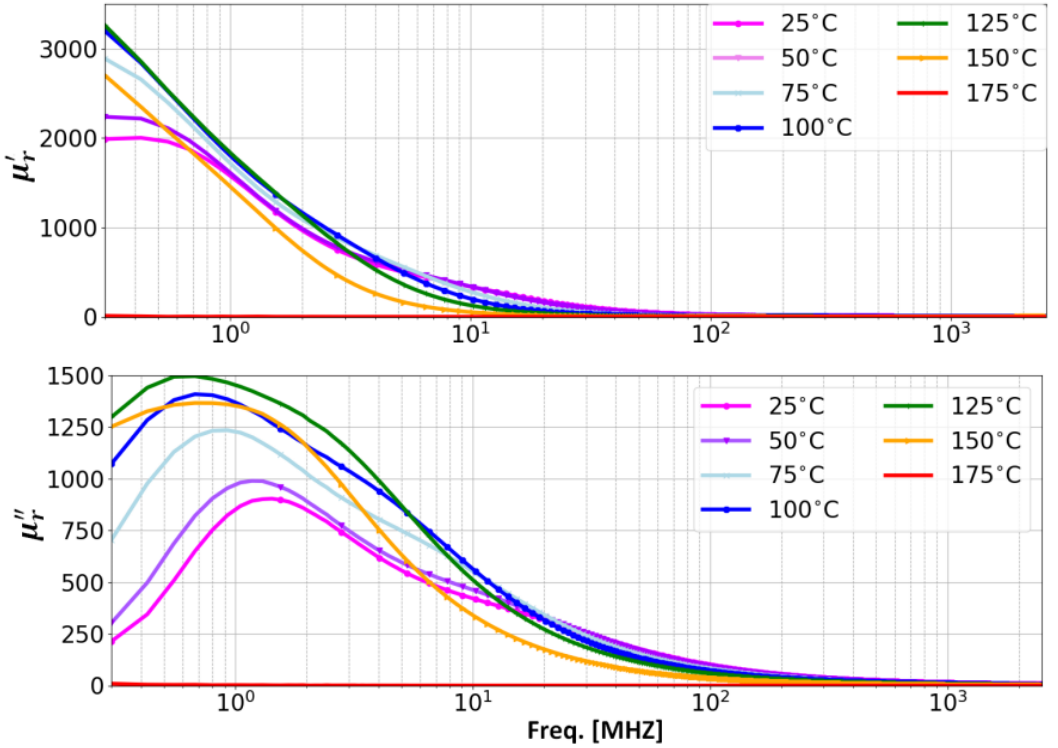

Chmielińska, A. *et al.* "Measurements of electromagnetic properties of ferrites as a function of frequency and temperature", In *Journal of Physics: Conference Series,* vol. 1067. No. 8, p. 082018. IOP Publishing.

Field response of the kicker magnet simulations

- **Field response** modelling (coupling Opera-2D with Cadence PSpice) to achieve required:
  - **Field rise time**
  - **Field flat-top quality**

Central cell inductance vs. frequency (Opera-2D)

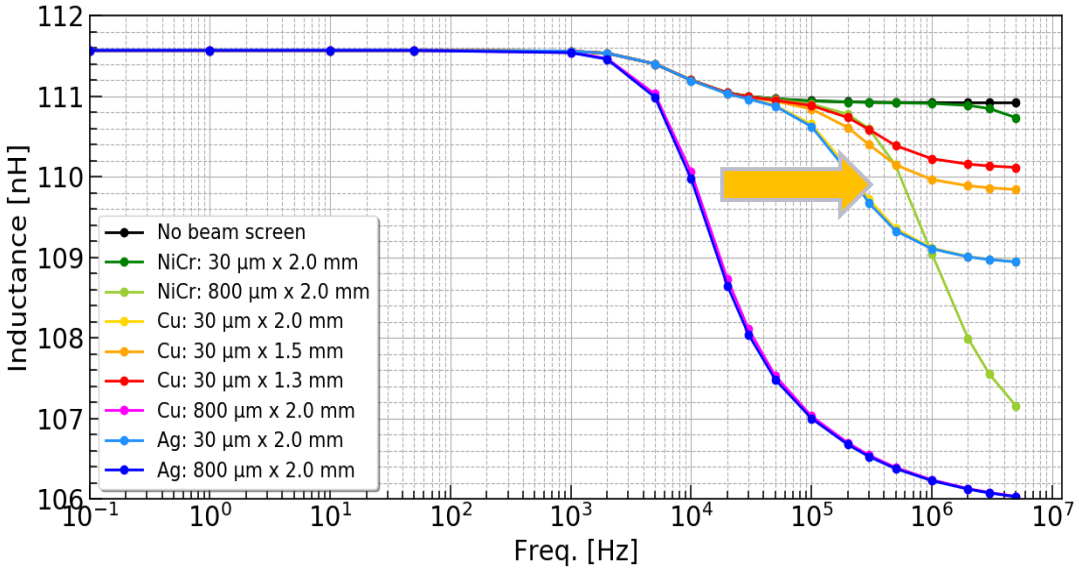

Selected baseline: Cu or Ag, 30 µm x 1.3 mm

Impact of a beam screen upon kicker waveform (PSpice)

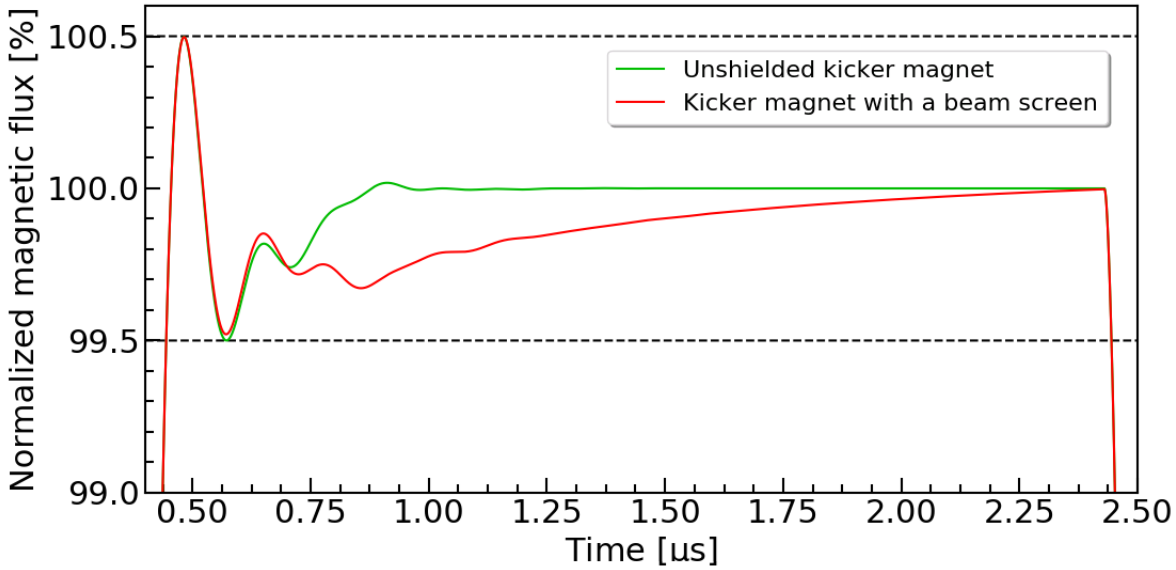

Proposed beam screen design satisfies the field rise time and the field flat-top quality requirements

Experimental benchmark

- **Coaxial-wire measurements** performed on the LHC MKI to validate numerical models (classical and resonant method)

Experimental setup

LHC MKI with a helical beam screen

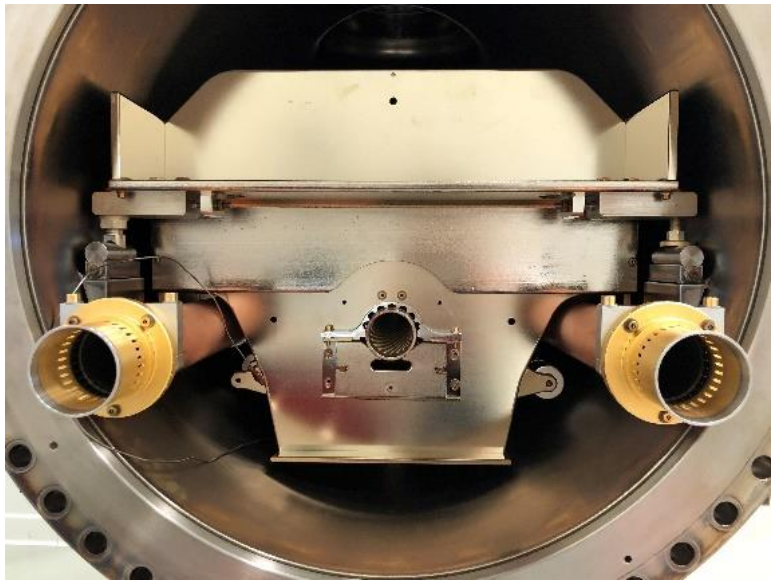

Longitudinal impedance

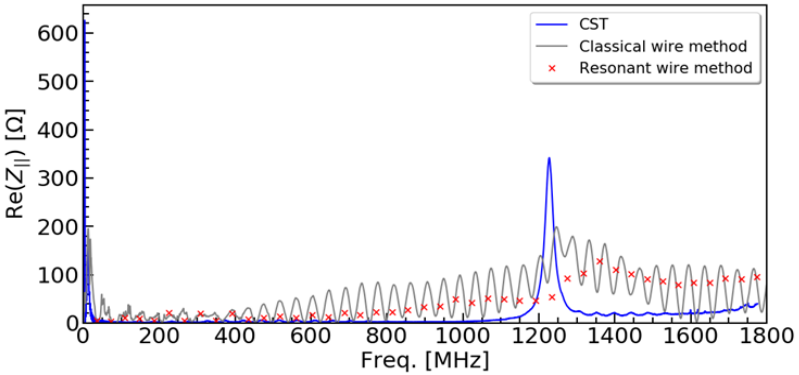

First demonstrated feasibility of this concept

Chmielińska, A. and Barnes, M. J. "Helical beam screen for the Future Circular Collider for hadrons injection kicker magnets." *Physical Review Accelerators and Beams* 23.4 (2020): 041002.

Measurements of beam coupling impedance

- **Coaxial-wire measurements** performed on the LHC MKI to validate numerical models (classical and resonant method)

Complete picture of the optimization of the beam screen design.

Consistent results in theoretical, numerical and experimental studies.

Chmielińska, A. and Barnes, M. J. "Helical beam screen for the Future Circular Collider for hadrons injection kicker magnets." *Physical Review Accelerators and Beams* 23.4 (2020): 041002.

Fellow in TE-MSC-TM (2020-2023)

Integration of numerical models with magnetic measurement data to model and characterize the magnetic field of superconducting magnets

- **Design of experiments** (test plan, specification of cycles)
- **Data-driven updates** of numerical models
- **Magnetic-field prediction** for machine operation (FiDeL)
  - Semi-empirical model decomposition
- **Software design** and **implementation** for data-analysis

Operational cycle of MCBC (vdM scans)

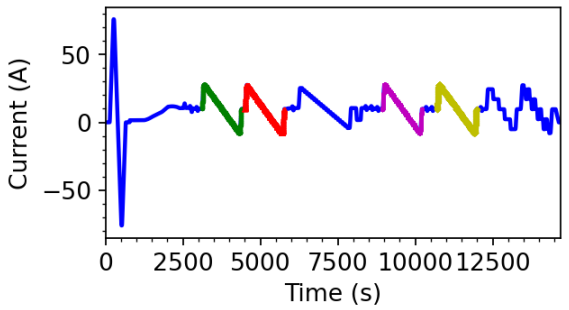

Cross-talk simulations in ROXIE

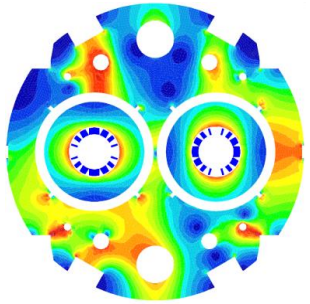

Rotating-coil measurements in SM18

PyMagAnalysis

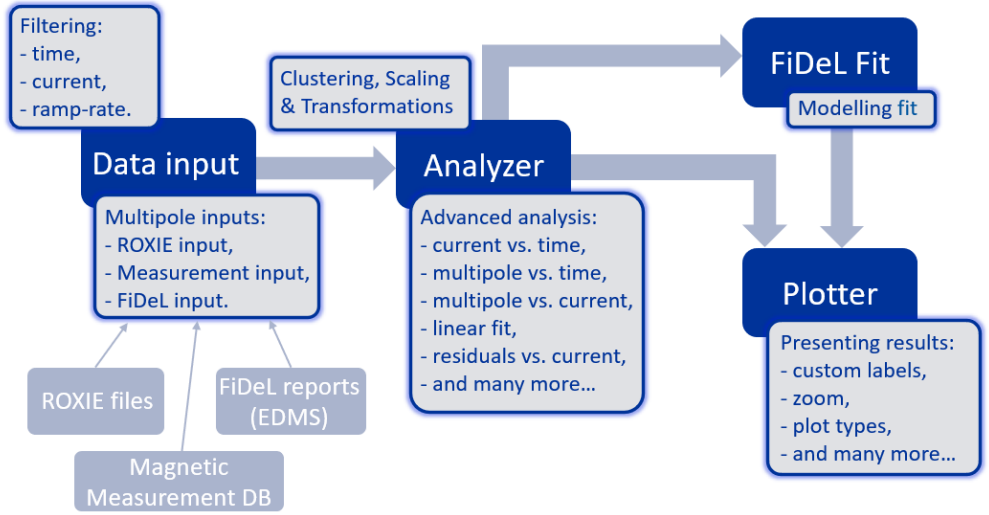

python GitLab SWAN jupyter

https://gitlab.cern.ch/te-msc-mm/pymaganalysis

Analysis of simulations and measurements to predict the magnetic field for the operation of superconducting magnets

FiDeL model for machine operation (I)

- The **Field Description of the LHC (FiDeL)** is the magnetic field prediction system that provides a model of the transfer function of magnetic circuits installed in the machine in order to retrieve the current level given the required field:

  → indispensable for LHC operation

  → uses parametric equations to fit **magnetic measurements**

  → based on **physical decomposition** of effects that contribute to the total field in the aperture of the magnet

  → uses **several levels of approximations**, starting from a linear dependance on the current and adding correction terms (depending on the magnet type and function).

FiDeL model for machine operation (II)

1. Geometric: $B_m^{\mathrm{geo}} = \gamma_m I.$

2. Magnetization: $B_m^{\mathrm{mag}} = \mu_m |I| \left(\frac{I_{\mathrm{inj}}}{|I|}\right)^{2-p_m} \left(\frac{I_{\mathrm{c}} - |I|}{I_{\mathrm{c}} - I_{\mathrm{inj}}}\right)^{q_m} \left(\frac{{T_{\mathrm{c0}}}^{1.7} - T^{1.7}}{{T_{\mathrm{c0}}}^{1.7} - {T_{\mathrm{meas}}}^{1.7}}\right)^{h_m}.$

3. Saturation: $B_m^{\mathrm{sat}} = \sum_{i=1}^{N} \sigma_m^i \, I\Sigma\left(I, S_m^i, I_{0m}^i, I_{\mathrm{nom}}\right),$

where $\Sigma(I, S, I_0, I_{nom}) = -\frac{1}{2}\left[1 + \mathrm{erf}\left(S\left(\frac{|I| - I_0}{I_{\mathrm{nom}}}\right)\right)\right], \mathrm{erf}(x) = \frac{2}{\sqrt{\pi}} \int_0^x e^{-t^2} dt.$

The fitting parameters are implemented in the LHC control system.

PyMagAnalysis

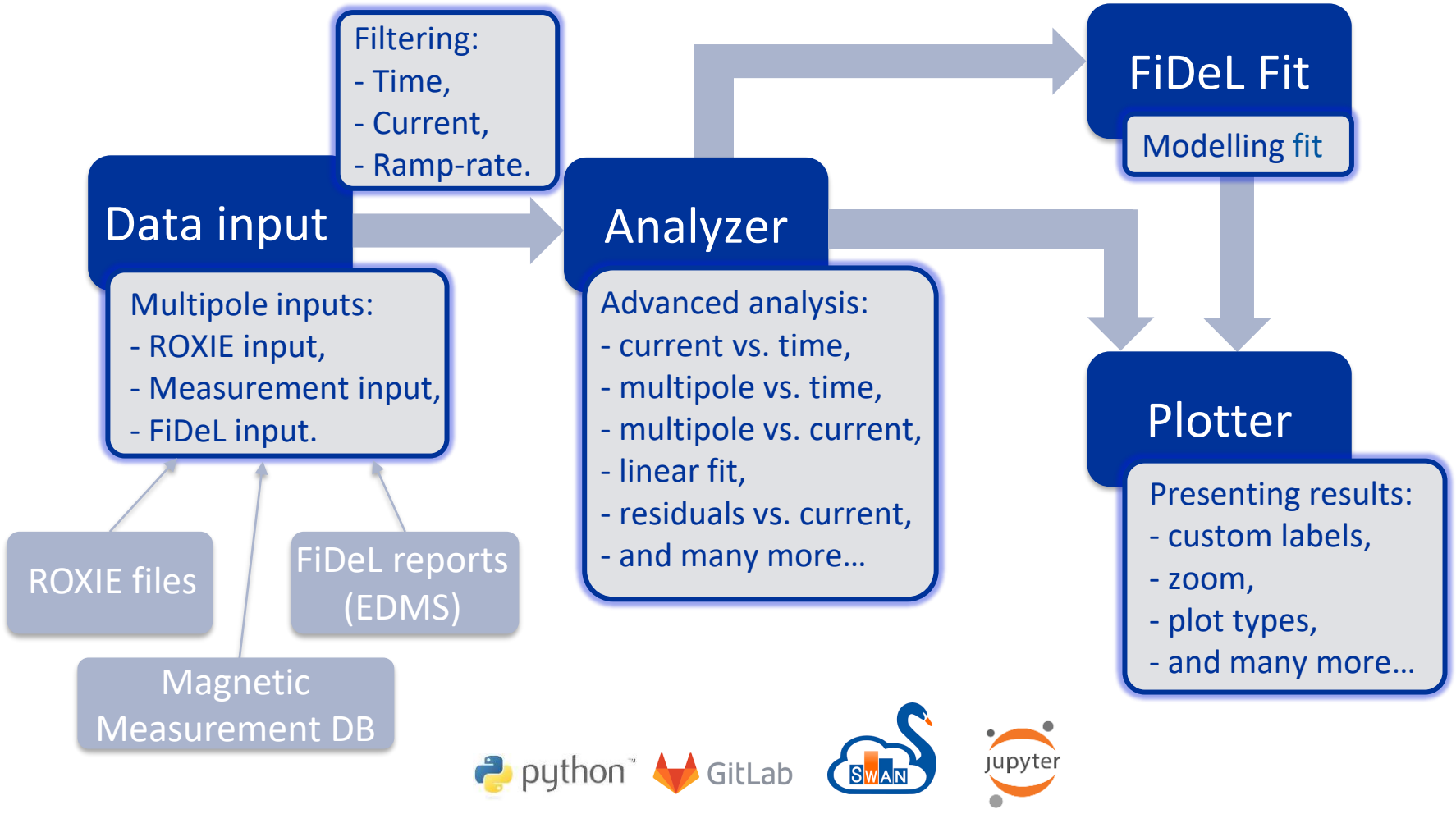

https://gitlab.cern.ch/te-msc-mm/pymaganalysis

Analysis of nonlinear effects during luminosity calibration (I)

- MCBC/MCBY magnets are used to provide beam separation during van der Meer (vdM) scans.

MCBC

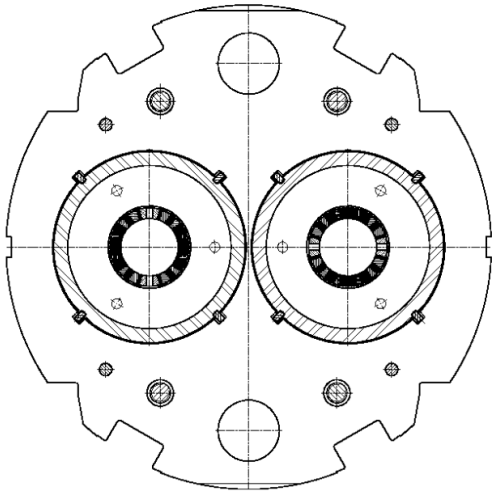

MCBY

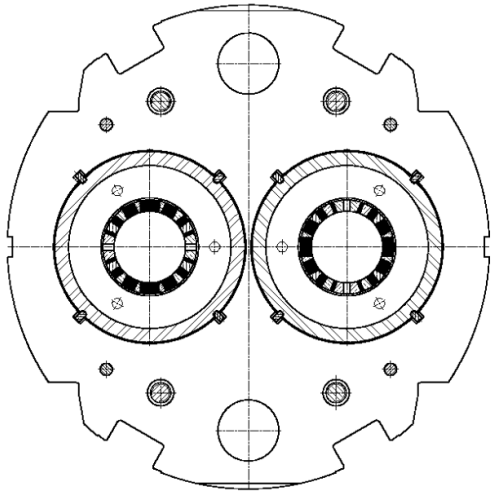

Operational cycles

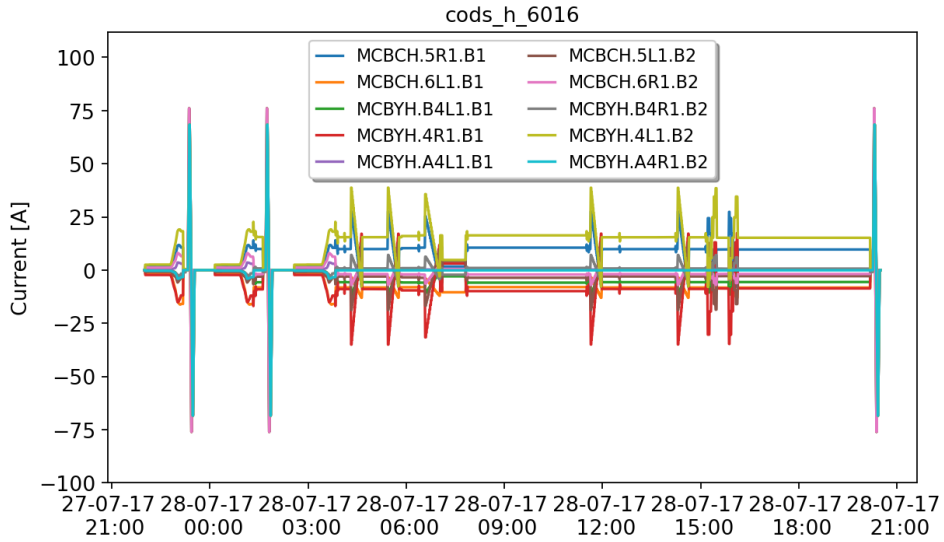

- **Nonlinearities** and **lack of repeatability during vdM scans** triggered the necessity to review the **hysteretic behaviour** of MCBC/MCBY magnets.

Measurements in SM18

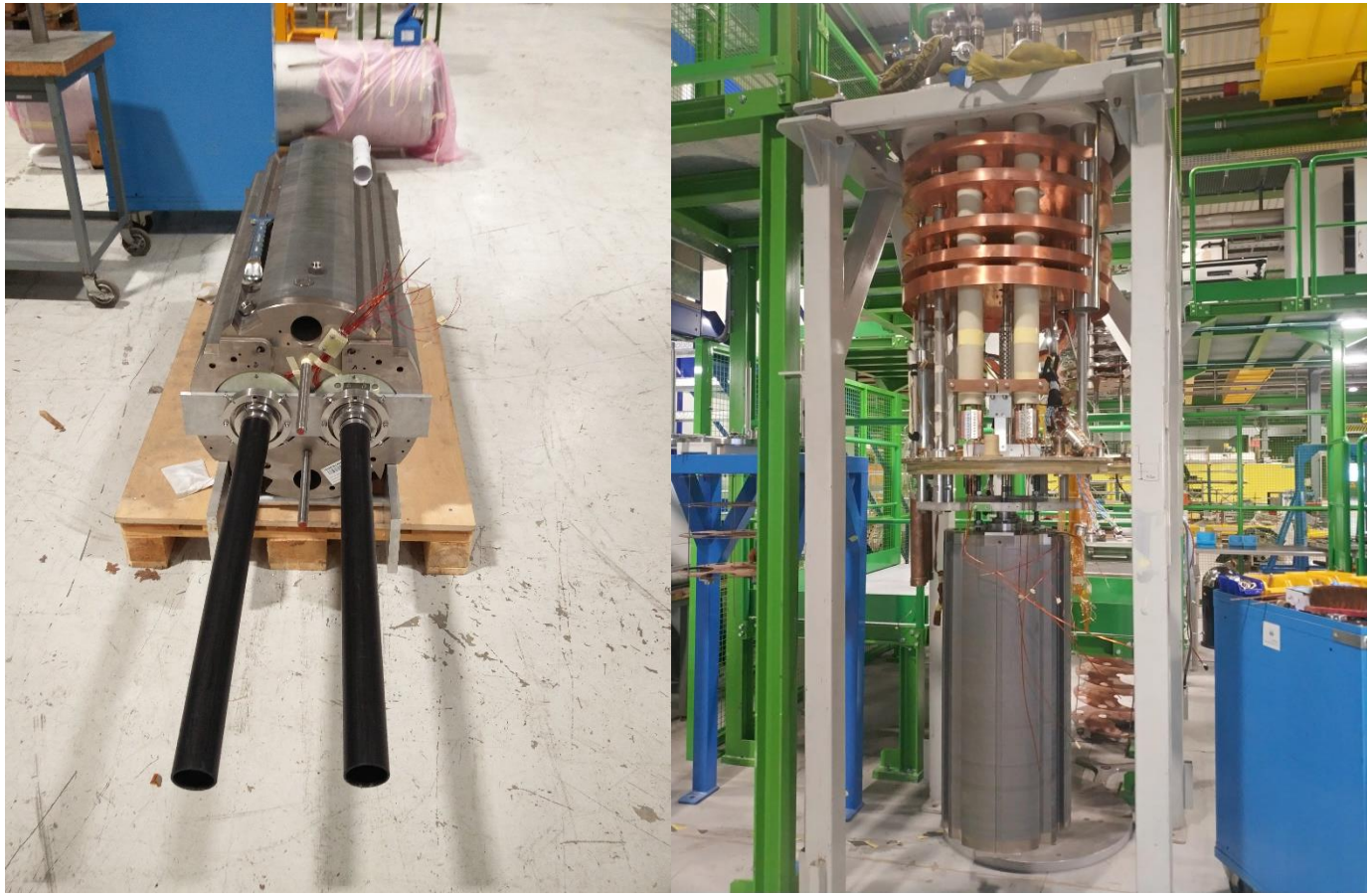

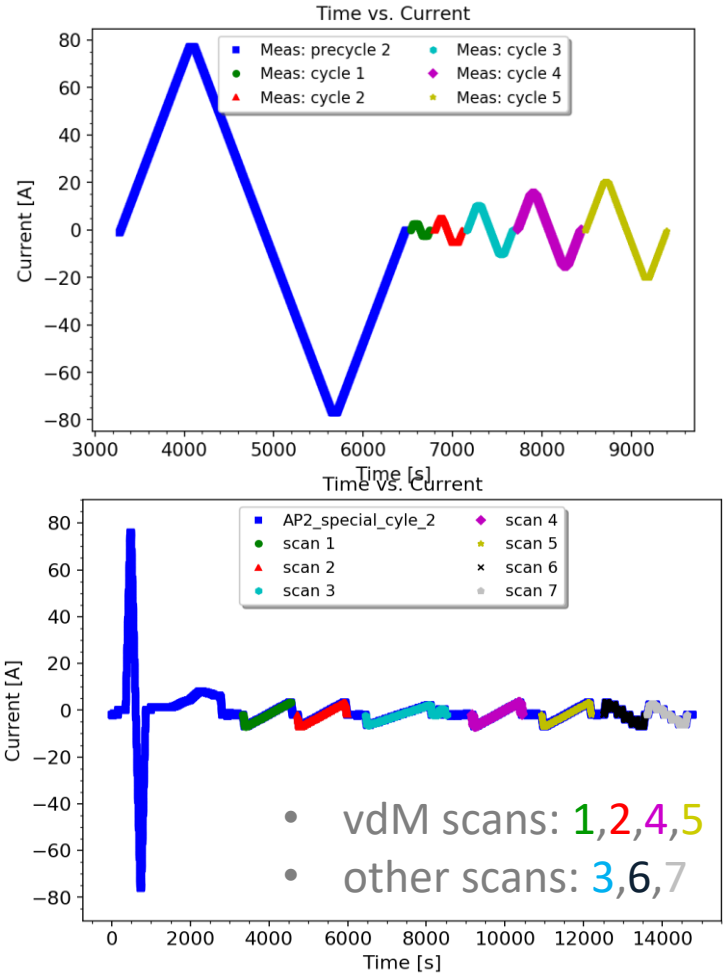

Extensive program of **standard** and **operational test cycles launched** to characterize the magnetic field and its **reproducibility from scan to scan** using the **rotating-coil technique.**

Analysis of measurements and simulations (I)

Analysis of nonlinear effects due to persistent currents

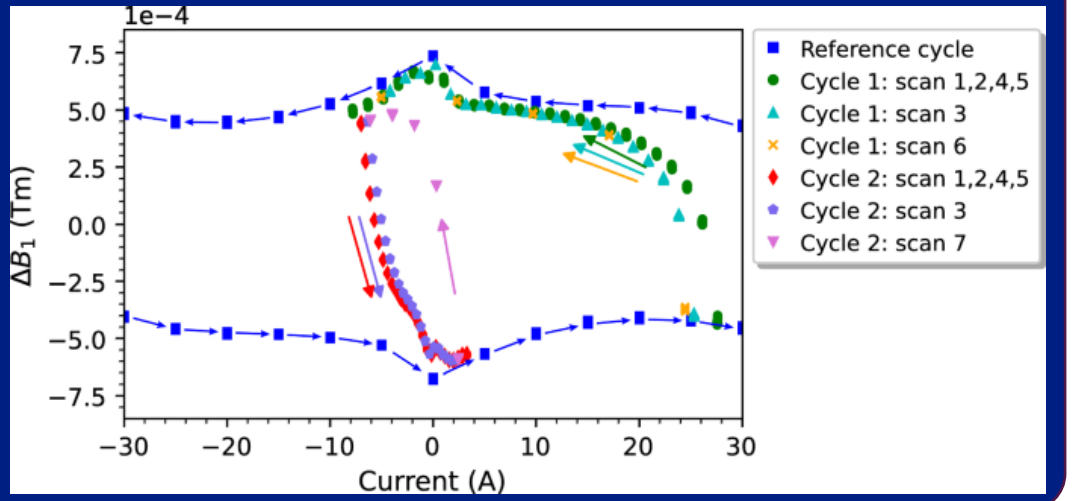

Update of the ROXIE models

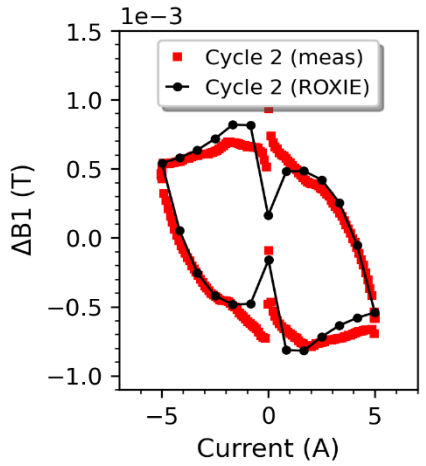

FiDeL model + beyond

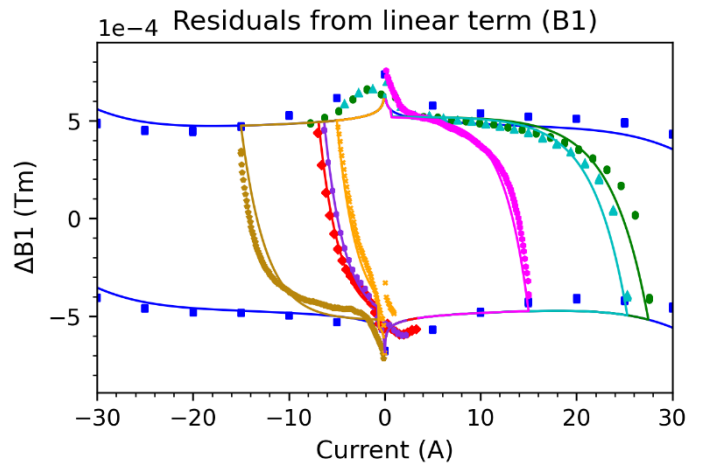

Developed numerical model to account for transitions between major magnetization branches

Benchmark of the proposed model

Comparison of the measured magnetization-branch transitions (markers) and the proposed extended FiDeL model for the MCBC magnet (dashed lines).

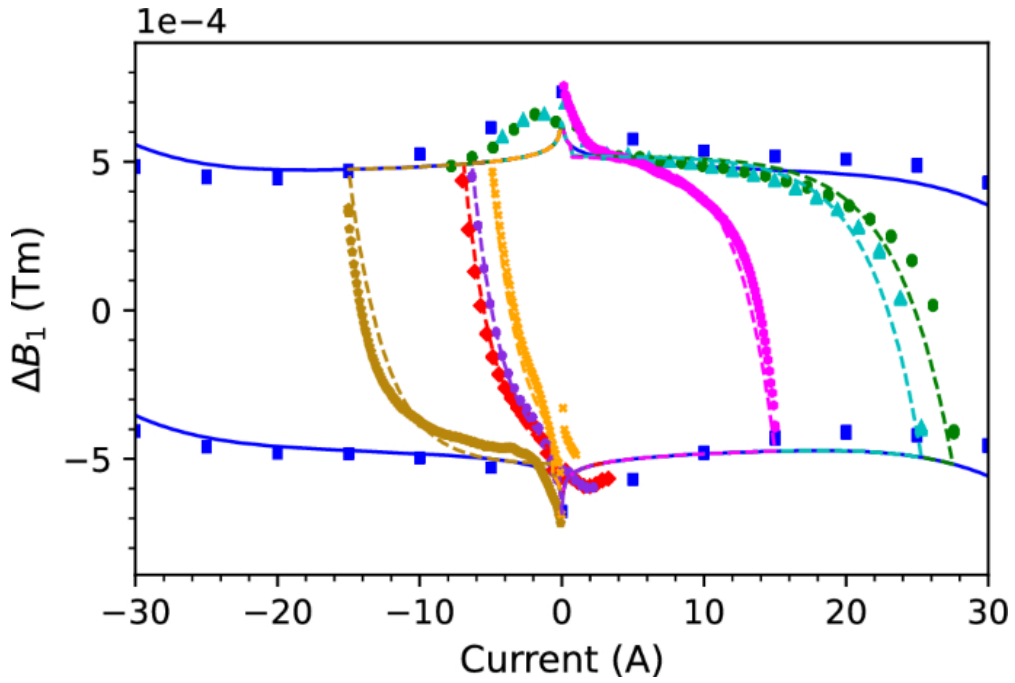

Predicted and measured impact of magnetic hysteresis on the transverse displacement

Courtesy of M. Hostettler

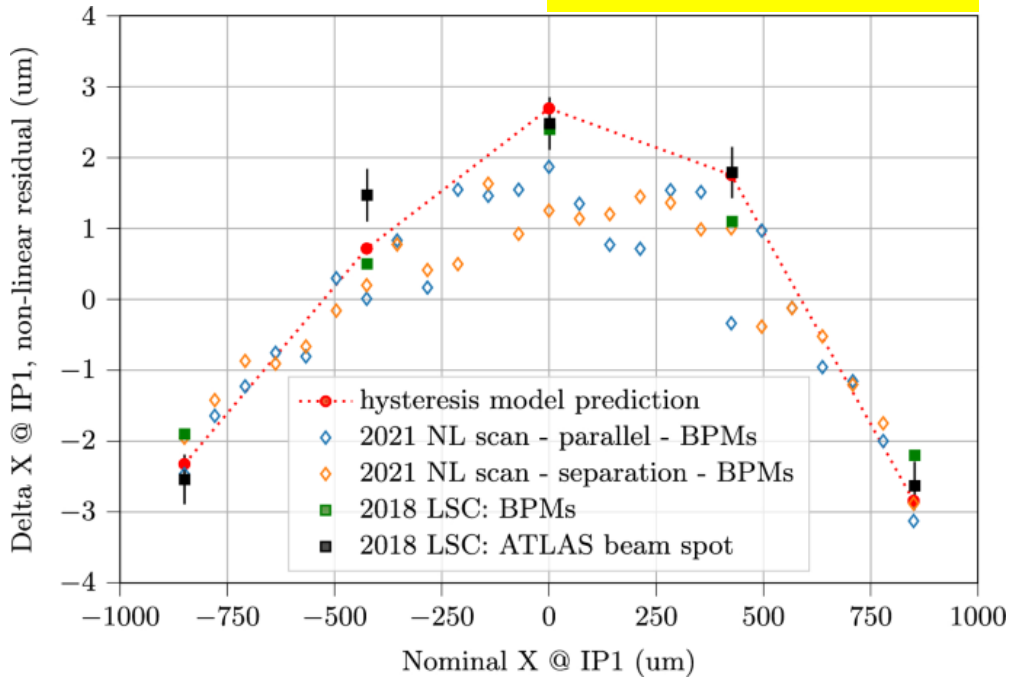

Chmielińska, A., et al. "Magnetization in superconducting corrector magnets and impact on luminosity–calibration scans in the Large Hadron Collider." *Eur. Phys. J. Plus* (2023) 138: 796.

Magnetic model for the MCBXF (I)

MCBXF

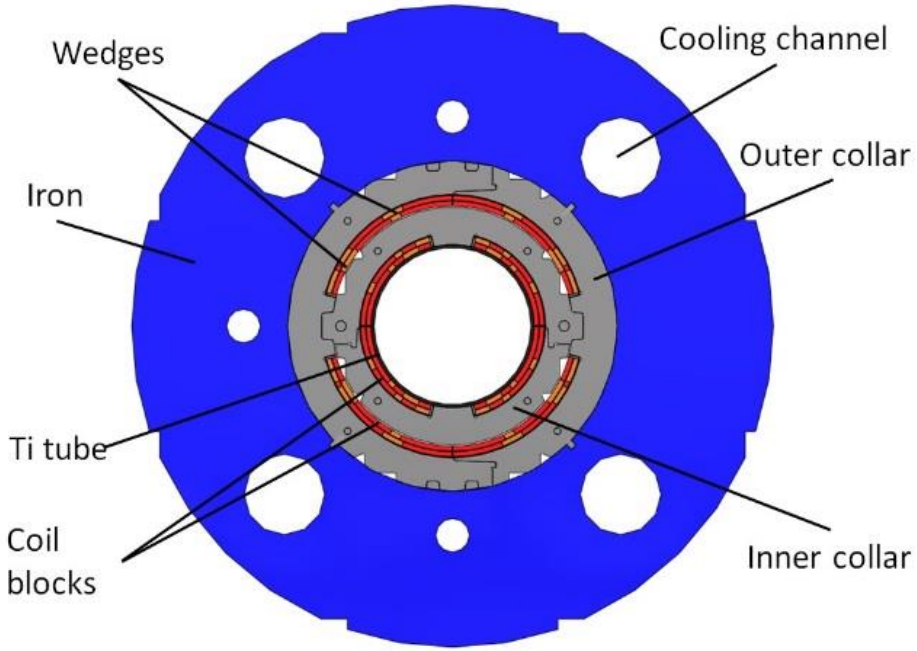

Powering cycles

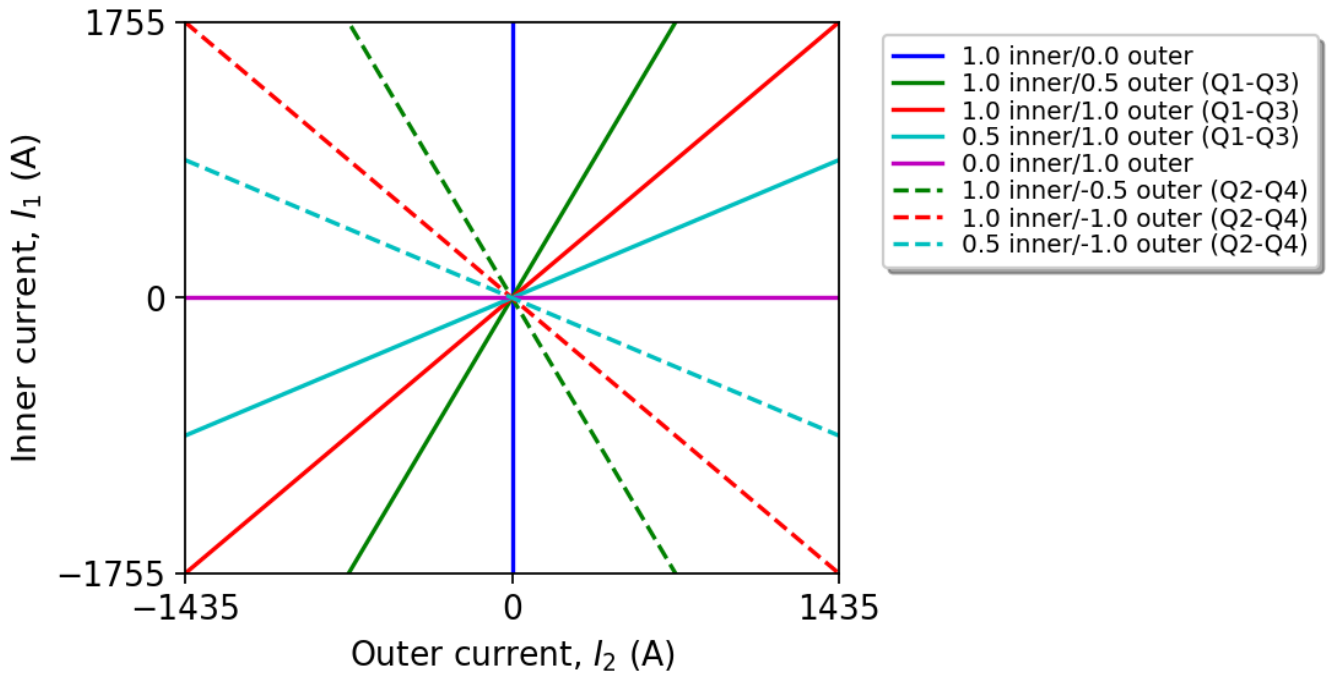

Inner coil provides vertical field
(main field B1, normal)

Outer coil provides horizontal field
(main field A1, skew).

Identifying the problem

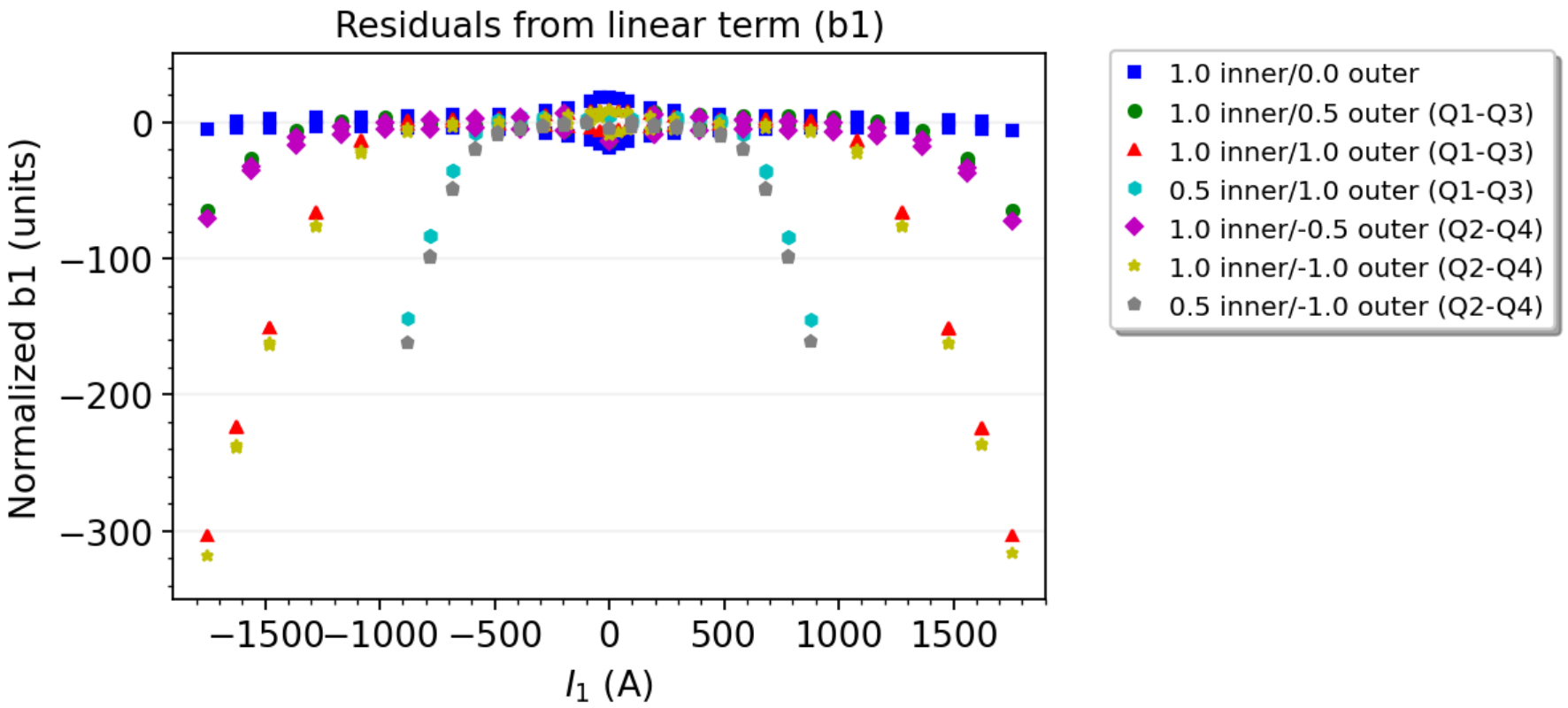

The development of FiDeL model is particularly challenging due to angular dependence of saturation (and persistent current magnetization).

Proposed model (I)

Original definition:

$$B_m^{\mathrm{sat}}(I_1) = \sum_{i=1}^{N} \sigma_m^i \, I_1 \Sigma\left(I_1, S_m^i, I_{0m}^i, I_{\mathrm{nom}}\right), \text{ where: } \Sigma(I, S, I_0, I_{\mathrm{nom}}) = -\frac{1}{2}\left[1 + \mathrm{erf}\left(S\left(\frac{|I| - I_0}{I_{\mathrm{nom}}}\right)\right)\right],$$

m – multipole, $\sigma_m, S_m, I_{0m}, I_{\mathrm{nom}}$ – fitting parameters.

Proposal:

$$B_m^{\mathrm{sat}}(I_1) \mapsto B_m^{\mathrm{sat}}(I_1, I_2)$$
$$A_m^{\mathrm{sat}}(I_2) \mapsto A_m^{\mathrm{sat}}(I_1, I_2)$$

I_1 - inner current
I_2 - outer current

$$B_m^{\mathrm{sat}}(I_1, I_2) = \sum_{i=1}^{N} \sigma_m^i \, I_1 G_m^B(I_1, I_2) \Sigma\left(I_1 G_m^B(I_1, I_2), S_m^i, I_{0m}^i, I_{\mathrm{nom\_1}}\right),$$
$$A_m^{\mathrm{sat}}(I_1, I_2) = \sum_{i=1}^{N} \sigma_m^i \, I_2 G_m^A(I_1, I_2) \Sigma\left(I_2 G_m^A(I_1, I_2), S_m^i, I_{0m}^i, I_{\mathrm{nom\_2}}\right),$$

where $G_m(I_1, I_2)$ is a function of inner and outer current (determined experimentally).

Proposed model (II)

Input: I_1, I_2

$$B_m^{\text{sat}}(I_1, I_2) = \sum_{i=1}^{N} \sigma_m^i \, I_1 \overbrace{\left(\frac{a}{\alpha(I_1, I_2) + \Delta} + b\right)}^{G_m^B(I_1, I_2)} \Sigma\left(I_1 \overbrace{\left(\frac{a}{\alpha(I_1, I_2) + \Delta} + b\right)}^{G_m^B(I_1, I_2)}, S_m^i, I_{0m}^i, I_{\text{nom1}}\right),$$

$$A_m^{\text{sat}}(I_1, I_2) = \sum_{i=1}^{N} \sigma_m^i \, I_2 \overbrace{\left(\frac{a}{\frac{\pi}{2} - \alpha(I_1, I_2) + \Delta} + b\right)}^{G_m^A(I_1, I_2)} \Sigma\left(I_2 \overbrace{\left(\frac{a}{\frac{\pi}{2} - \alpha(I_1, I_2) + \Delta} + b\right)}^{G_m^A(I_1, I_2)}, S_m^i, I_{0m}^i, I_{\text{nom2}}\right)$$

where: $\alpha(I_1, I_2) = \tan^{-1}\left(\frac{|I_1|/I_{\text{nom1}}}{|I_2|/I_{\text{nom2}}}\right)$

Modelling error

New model with angular dependence of saturation

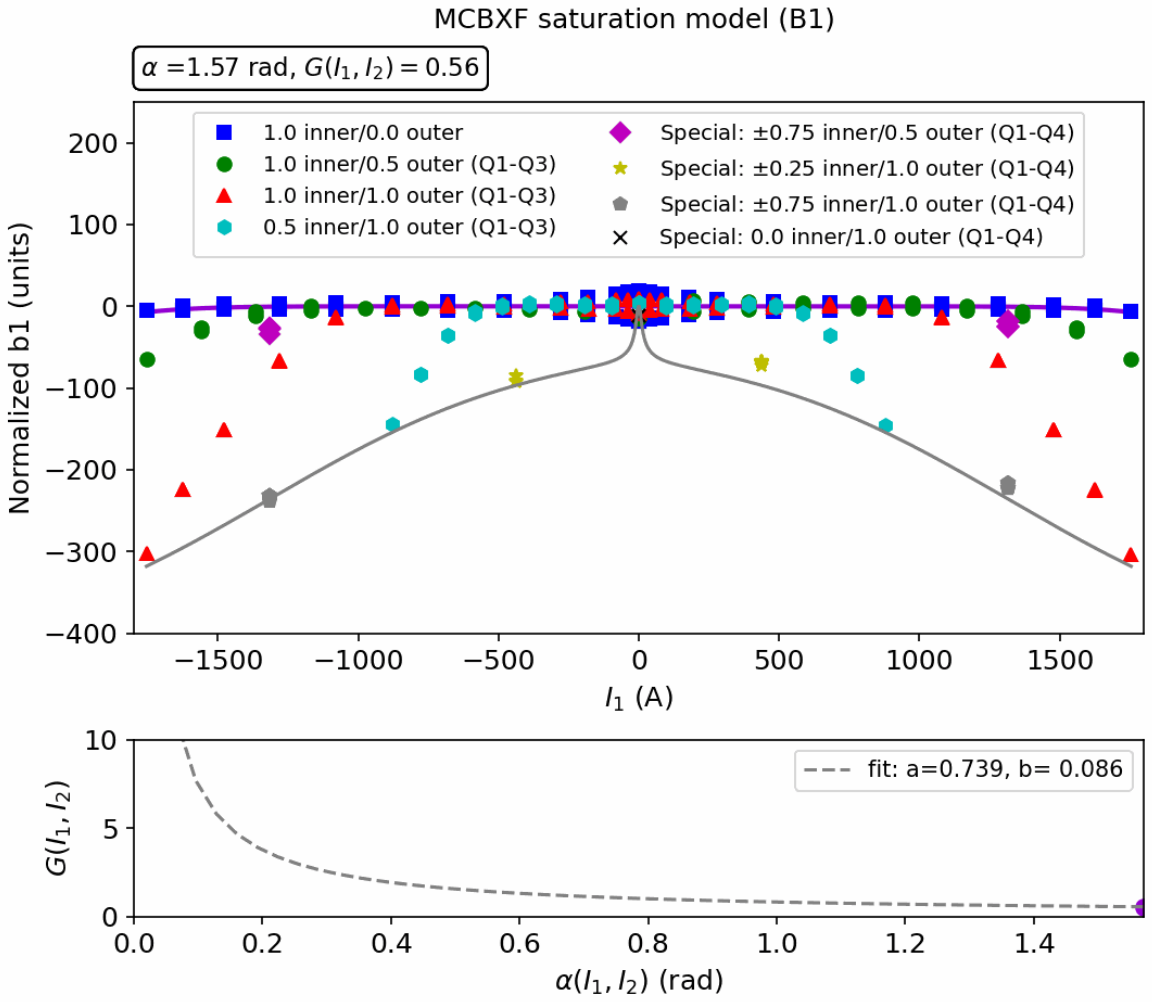

The error is within required specification (±30 units for B1/A1)

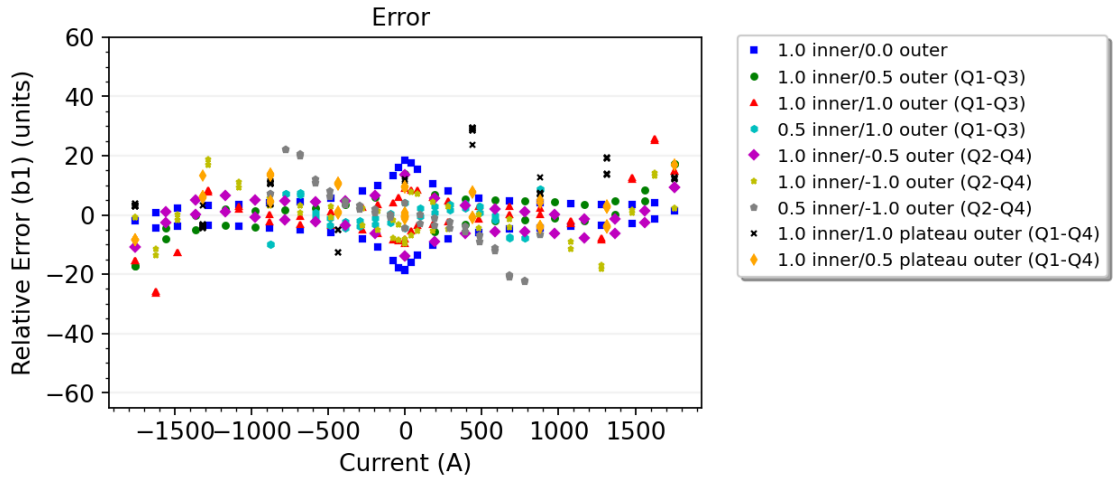

Baseline for HL-LHC

Modelling error

New model with angular dependence of saturation

With **PyMagAnalysis** framework we brought **the best available knowledge** from **simulations** and **measurements** to **understand the magnet behavior itself** and to provide **precise field predictions for operation**.

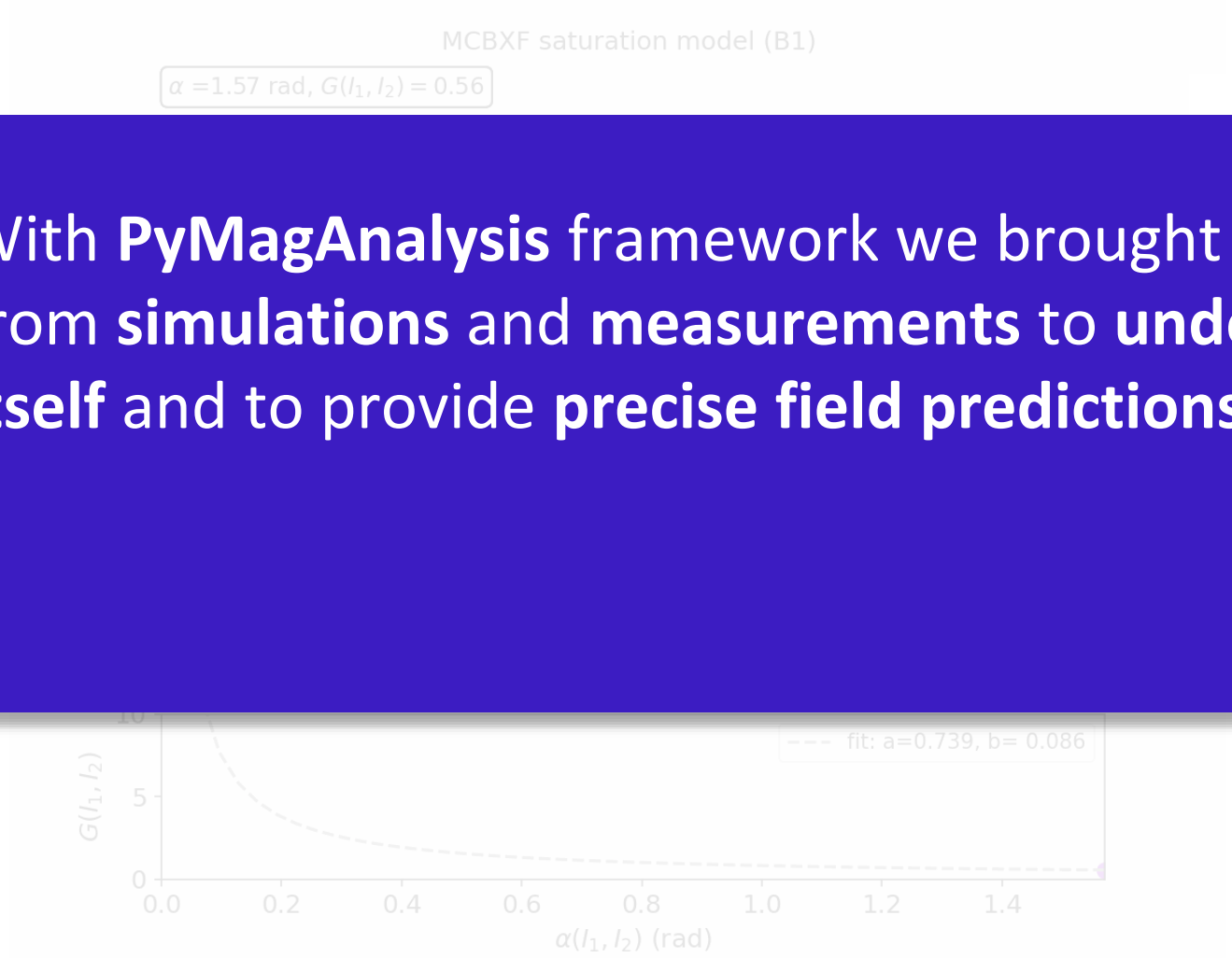

Error

Baseline for HL-LHC

Thank you for your attention!

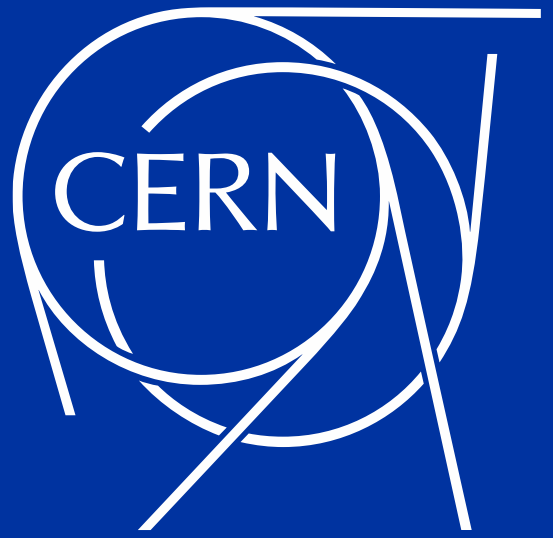
CERN